

## MODELING OF THIN, BACK-WALL SILICON SOLAR CELLS

Cosmo R. Baraona  
National Aeronautics and Space Administration  
Lewis Research Center

### SUMMARY

The performance of silicon solar cells with p-n junctions on the nonilluminated surface (i.e., upside-down or back-wall cells) was calculated. These structures consisted of a uniformly shaped p-type substrate layer, a p<sup>+</sup>-type field layer on the front (illuminated) surface, and a shallow, n-type junction on the back (nonilluminated) surface. A four-layer solar cell model was used to calculate efficiency, open-circuit voltage, and short-circuit current. The effect on performance of p-layer thickness and resistivity was determined. The diffusion length was varied to simulate the effect of radiation damage. The results show that peak initial efficiencies greater than 15 percent are possible for cell thicknesses of 100 micrometers or less. After 10 years of radiation damage in geosynchronous orbit, thin (25 to 50  $\mu\text{m}$  thick) cells made from 10- to 100-ohm-cm material show the smallest decrease (~10 percent) in performance.

### INTRODUCTION

A back-wall, or upside-down, solar cell (ref. 1) is a conventional n<sup>+</sup>-p-p<sup>+</sup> device with its collecting p-n junction on the nonilluminated bottom side of the device. The p<sup>+</sup> side is covered with a gridded contact; the n<sup>+</sup> region has full area metallization. Back-wall cells are similar to certain high-voltage cell designs that have collecting p-n junctions 25 or more micrometers from the illuminated surface (ref. 2) or to interdigitated back-contact cells (refs. 3 and 4). The interdigitated cells that are most similar to the back-wall cell design are those with a front-surface field. Structures like these have been prepared for space use; hence, it is of interest to assess their performance in a radiation environment.

The present work explores analytically the performance of a range of back-wall cell structures. The performance trends of these back-wall cell designs are calculated by using a four-layer solar cell model. This model has been used previously (refs. 5 to 8) to calculate solar cell performance and has shown good agreement with experiment. The influence of the back-wall cell thickness, the bulk resistivity, and the radiation damage coefficient on performance was determined. The ranges of parameters used in the model can be achieved with present technology. These calculations are intended to give the scope of the problem and to illustrate performance trends. Experimental data were not available for comparison.

## THEORETICAL MODEL

The solar cell model used for these calculations has been described elsewhere (refs. 5 to 8). The model is based on a four-layer, homojunction semiconductor solar cell. Layer widths, impurity concentrations, surface properties, and material properties can be specified. Exponential impurity distributions are assumed so that drift field strengths within each layer are constant.

The equations used in the model were derived by solving the continuity equation: The current transport equation and appropriate boundary conditions were used to solve for the diode saturation current density  $J_0$  and for the short-circuit current density  $J_{sc}$ . The open-circuit voltage  $V_{oc}$ , maximum power  $P_{max}$ , curve factor CF, and air-mass-zero (AMO) efficiency were calculated in reference 8. In calculating the curve factor, a diode quality factor of 1 and a series resistance of zero were assumed. For most cells, this represents about a 3 percent overestimate of power and curve factor. Data in this paper were not adjusted for that overestimate. The AMO solar constant used was 135.6 mW/cm<sup>2</sup>.

Some of the values used in the calculations are shown in figure 1. Zero optical reflection and lower front-surface recombination velocity ( $S \leq 10$  cm/sec) were used to improve cell performance. The p<sup>+</sup> front-surface field region was about 1 micrometer deep. The carrier concentration, mobility, and diffusion length were characteristic of an alloyed or heavily doped diffused region. The n<sup>+</sup> and n regions were 0.25 micrometer deep and had properties characteristic of a shallow diffused junction. The surface recombination velocity at the back wall (under the full-area metallization) was 10<sup>8</sup> cm/sec.

Both front- and back-surface recombination velocities were assumed to be constant and independent of radiation fluence. If S increased with irradiation, additional degradation in cell performance would be predicted by the four-layer model. Complete collection of carriers was assumed within the depletion region.

The p-region bulk of the cell was a uniformly doped, field-free region from 25 to 100 micrometers thick. The p-region resistivities, corresponding to initial diffusion lengths and radiation damage coefficients for 1-MeV electrons (ref. 9) used in the calculations are shown in table I. The initial diffusion lengths chosen correspond to reasonable minority carrier lifetimes for the various resistivities. The diffusion length after a given fluence was calculated with the usual equation (ref. 9).

## RESULTS AND DISCUSSION

Efficiency is shown as a function of fluence for 25-, 50-, and 100-micrometer-thick, 10-ohm-cm back-wall cells in figure 2. Almost all the loss in efficiency is due to loss in  $J_{sc}$ . The initial unirradiated efficiencies are about 15.2 percent for 25- and 50-micrometer-thick cells and about 14.1 percent for 100-micrometer-thick cells. This demonstrated that high beginning-of-life (BOL) efficiencies are possible for back-wall cells. Figure 2 also shows that thin back-wall cells degrade less rapidly than thicker cells.

A fluence of  $4 \times 10^{14}$  electrons/cm<sup>2</sup> corresponds to about 10 years in geosynchronous orbit and is defined herein as the end-of-life (EOL) condition. At end of life the 25-micrometer-thick cell is 13.4 percent efficient and the 50- and 100-micrometer thick cells are 11.3 and 6.2 percent efficient, respectively. Thus, acceptable end-of-life efficiencies may be possible if back-wall cells are made ultrathin.

Similar calculations were performed for back-wall cells made from 1- and 100-ohm-cm material. These calculations, along with those for 10-ohm-cm cells, are shown in figure 3. Efficiency is plotted as a function of resistivity for three cell thicknesses. The beginning-of-life results (fig. 3(a)) show that 15 percent efficiencies can be achieved with several combinations of thickness and resistivity. However, 100-micrometer-thick cells made from 1- and 10-ohm-cm material are less efficient because the diffusion length is reduced. The end-of-life results (fig. 3 (b)) show that 50-micrometer-thick, 100-ohm-cm back-wall cells and 25-micrometer-thick, 10- and 100-ohm-cm back-wall cells can achieve an efficiency of 13 percent. This represents only about a 10 percent loss in performance over the life span, compared with 15 to 20 percent for conventional cell designs. Therefore, using thin, high-resistivity material appears to yield both high BOL and high EOL performances in the back-wall cell design.

#### SUMMARY OF RESULTS

Calculations of back-wall silicon solar cell performance with a four-layer model gave the following results:

1. Back-wall cells can achieve 15 percent air-mass-zero beginning-of-life efficiency.
2. Air-mass-zero, end-of-life efficiency of 13 percent is possible with 50-micrometer-thick, 100-ohm-cm material or with 25-micrometer-thick, 10- or 100-ohm-cm material.

#### REFERENCES

1. Brandhorst, H. W., Jr.: Back Wall Solar Cell. U.S. Patent 4,131,486, Dec. 1978.
2. Neugroschel, A.; and Lindholm, F.A.: Design of High Efficiency HLE Solar Cells for Space and Terrestrial Applications. Solar Cell High Efficiency and Radiation Damage - 1979. NASA CP-2097, 1979.
3. Carbajal, B. G.: High Efficiency Cell Development. (TI-03-79-16, Texas Instruments, Inc.; NASA Contract NAS7-100.) NASA CR-158581, 1979.
4. Anspaugh, Bruce E.; Miyahira, Tetsuo F.; and Scott-Monck, John A.: Electron Irradiation of Tandem Junction Solar Cells. Solar Cell High Efficiency and Radiation Damage - 1979. NASA CP-2097, 1979.
5. Wolf, M.: Drift Fields in Photovoltaic Solar Energy Converter Cells. Proc. IEEE, vol. 51, May 1963, pp. 674-693.

6. Godlewski, M. P.; Baraona, C. R., and Brandhorst, H. W., Jr.: The Drift Field Model Applied to the Lithium-Containing Silicon Solar Cell. Tenth Photovoltaic Specialists Conference, Institute of Electrical and Electronics Engineers, Inc., 1974, pp. 378-383.
7. Godlewski, M. P.; Baraona, C. R.; and Brandhorst, H. W., Jr.: Low-High Junction Theory Applied to Solar Cells. Tenth Photovoltaic Specialists Conference, Institute of Electrical and Electronics Engineers, Inc., 1974, pp. 40-49.
8. Baraona, C. R.; and Brandhorst, H. W., Jr.: Analysis of Epitaxial Drift Field N on P Silicon Solar Cells. Twelfth Photovoltaic Specialists Conference, Institute of Electrical and Electronics Engineers, Inc., 1976, pp. 9-14.
9. Srour, J. R.; et al.: Damage Coefficients in Low Resistivity Silicon. (NRTC-75-23R, Northrup Research and Technology Center, NASA Contract NAS3-17849.) NASA CR-134768, 1975.
10. Miyahira, T. F.; and Anspaugh, B.: Electron Radiation Degradation of Recent Solar Cell Designs. Thirteenth Photovoltaic Specialists Conference, Institute of Electrical and Electronics Engineers, Inc., 1978, pp. 463-464.

TABLE I. - BACK-WALL CELL MODELING PARAMETERS

Resistivity, ohm-cm	Initial diffusion length, $\mu\text{m}$	Damage coefficient, electron <sup>-1</sup>
1	100	$2.0 \times 10^{-10}$
10	200	$4.5 \times 10^{-11}$
100	600	$1.0 \times 10^{-11}$

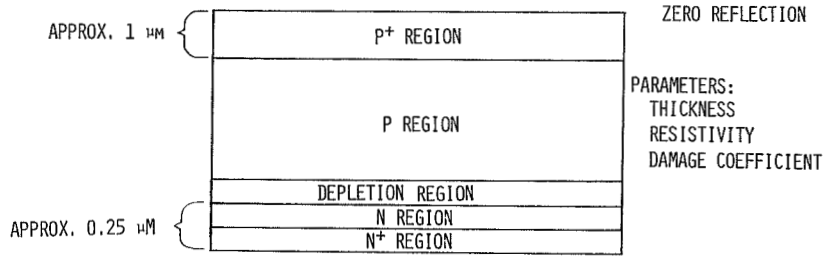


Figure 1.- Cross section of thin, four-layer backwall cell. Air-mass-0 illumination.

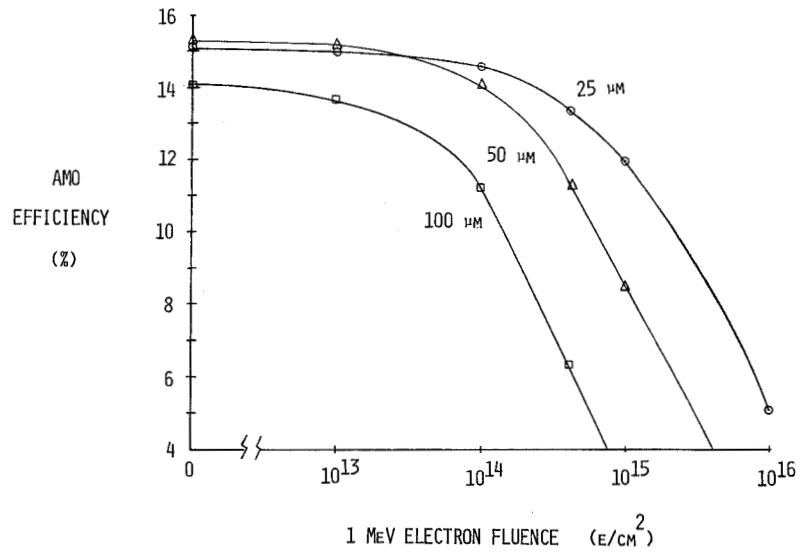


Figure 2.- Efficiency as function of fluence for 10-ohm-cm backwall cells.

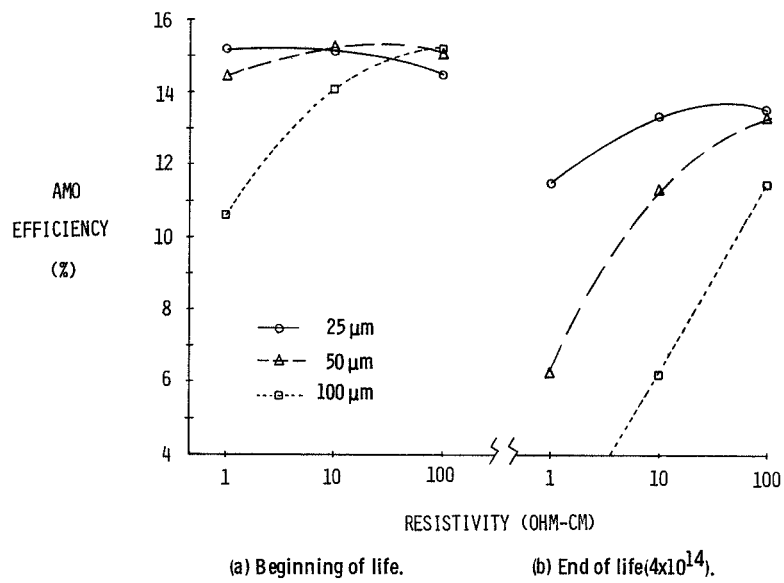


Figure 3. - Efficiency as function of resistivity for backwall cells.